Acta Cryst. (1957). **10**, 291

The Integral Transformations of Atomic Scattering Factors and their Applications

By Masao Atoji*

School of Chemistry, University of Minnesota, Minneapolis 14, *Minnesota, U.S.A.*

(*Received* 17 *April* 1956 *and in revised form* 1 *August* 1956)

The Fourier, Hankel and Gauss transformations of atomic scattering factors, expressed in analytical forms obtained from the electronic wave functions and from the Thomas–Fermi method, are discussed. These transformations, in three dimensions and in projection, are applied to observe the effect of thermal vibrations on the electron distribution in all atoms, in connection with the accuracy of atomic co-ordinates in the electron-density maps and with the series-termination effect in X-ray Fourier methods.

Some of the important results are as follows. All atomic scattering factors can be expressed in the closed form $\sum_n' H/(s^2+E)^n$, where E and H are independent of $s = 2 \sin \theta/\lambda$. The iso-electronic atoms such as F^- and $O^=$ may well be distinguishable from the peak values of the electron-density distribution. The Thomas–Fermi method is found to be a satisfactory approximation even for the lighter atoms, provided that their thermal vibrations are large. The following relation between the peak height, $\varrho_n(0)$, and the peak curvature, $\varrho_n''(0)$, may be useful for the refinement of the temperature factor

$$16\pi^2 \partial \varrho_n(0)/\partial B = n\varrho_n''(0) ,$$

where n is the dimension of the projection. The possibility for the determination of the characteristic temperature, using the electron-density data from X-ray methods, is suggested. The agreement between the observed and calculated values of the electron-density function is quite reasonable.

1. Introduction

It is our hope to contribute to the theory of molecular structure by reproducing precisely the electron distribution of atoms in X-ray Fourier maps. Efforts have been made to elucidate the electron density not only of the hydrogen atom but also of valence electrons. However, the electron density of an atom at rest may not be obtained experimentally even at the absolute zero temperature, because of its zero-point vibrations. Nevertheless, from the knowledge of these vibrational effects, one may deduce information useful to molecular theories and to lattice dynamics.

In the present paper, the electron density of an atom is expressed by the Fourier, Hankel and Gauss (or simply Fourier–Hankel–Gauss) transformations of the atomic scattering factor modified by the Debye–Waller temperature factor. All atomic scattering factors are expressed in analytical forms using either the electronic wave functions or the Thomas–Fermi (TF) method. Since reliable data on the valence-electron density in the X-ray Fourier maps are not available, most of the present numerical results are given for the peak values of the electron density. However, the equations for the valence electrons are given in their general forms.

Higgs' treatment on the carbon atom (1953) was directed along the same line, although the methods of transformation and some of the results in the present paper are different and are readily applicable to all atoms. McDonald's paper on the hydrogen atom (1956) appeared recently. Since some additional results were obtained, the hydrogen atom will also be discussed here as a special case.

2. Analytical forms of the atomic scattering factors

The atomic scattering factor is expressed by

$$f(s) = \int_0^\infty 4\pi r^2 \varrho(r) \frac{\sin 2\pi sr}{2\pi sr} dr , \qquad (1)$$

where $\varrho(r)$ is the radial electron density and is assumed to have spherical symmetry, r is the distance in crystal space in Å and $s = 2 \sin \theta/\lambda$ is the distance in reciprocal space in $Å^{-1}$. θ is the Bragg reflection angle and λ is the wavelength of the radiation in Å.

The Slater wave functions (Slater, 1930; Duncanson & Coulson, 1944) and Pauling's hydrogen-like wave functions (Pauling & Sherman, 1932) both give, in general, a radial density function of the form,

$$\varrho(r) = \Sigma k r^n \exp(-cr) , \qquad (2)$$

where the values of k, n and c depend on both the quantum number of the electron and the form of the

* Present address: Institute for Atomic Research and Department of Chemistry, Iowa State College, Ames, Iowa, U.S.A.

wave function chosen. The f-factor for the radial density distribution of $kr^n \exp(-cr)$ is*

$$f(s) = \frac{2\{(n+1)!\}k \sin\{(n+2)\arctan(2\pi s/c)\}}{s(4\pi^2 s^2+c^2)^{n/2+1}}, \quad (4)$$

where n is an integer. Equation (4) can also be expressed in a finite-series form as

$$f(s) = \frac{2\{(n+1)!\}k}{s}\left\{\frac{c}{4\pi^2 s^2+c^2}\right\}^{n+2} \times \sum_{0\le 2m\le n+1} (-1)^m \binom{n+2}{2m+1}\left(\frac{2\pi s}{c}\right)^{2m+1}, \quad (5)$$

where $\binom{n+2}{2m+1}$ is the binomial coefficient. It may be noted that the results of Pauling & Sherman (1932) and of McWeeny (1951) can be summarized by equation (5). In particular, if $n = 0$, equations (4) and (5) are for the hydrogen-like atom.

For heavy atoms, the TF method may be used. Applying the Rozental-approximation formulae to the TF function (Rozental, 1935), Umeda (1951) obtained

$$f(s) = Z^{5/3} \sum_n \frac{\alpha_n \beta_n}{s^2+\beta_n Z^{2/3}}, \quad (6)$$

where Z is the atomic number and $\sum_n \alpha_n = 1$. The constants without units are:

$$\alpha_1 = 0{\cdot}255, \quad \beta_1 = 0{\cdot}006984,$$
$$\alpha_2 = 0{\cdot}581, \quad \beta_2 = 0{\cdot}10348,$$
$$\alpha_3 = 0{\cdot}164, \quad \beta_3 = 2{\cdot}1896,$$

from the Rozental three-term approximation.

f_A and f_T, obtained respectively from the electronic wave functions and from the TF method, are closely related to each other, namely,

$$\sum_n C_n \frac{\partial^n f_T}{\partial p^n} = f_A, \quad (7)$$

where p is $\beta_n Z^{2/3}$ and C_n's are operational factors. In other words, all f-factors may be reasonably expressed by

$$f(s) = \sum_n \frac{H}{(s^2+E)^n}, \quad (8)$$

where H and E are independent of s.

The best f-factor calculated from the Hartree and Hartree–Fock equations is now becoming available for many atoms (Berghuis *et al.*, 1955), but only numerically. However, it is possible to derive analytical expressions for any of these f-factors by means of Slater's analytical functions (Slater, 1932; Löwdin, 1953). Since Slater's function is a linear combination of the hydrogen-like wave functions as in (2), the f-factors can similarly be expressed by (4), (5) and (8).

Instead of equation (8), it is possible to find other functions which are good approximations to the best f-factor. If McWeeny's Gaussian approximation to the electronic wave function (1953) is employed, the f-factor is expressed by a linear combination of the parabolic cylinder function (Whittaker & Watson, 1935, p. 347). The function, $(\tanh x)/x$ may be used similarly. For example, the Hartree f-value of Na^+ is approximated by $10(\tanh 2{\cdot}5s)/(2{\cdot}5s)$ with fair accuracy. Although these curve-fitting methods have less generality, they often avoid tedious mathematical treatment.

3. The Fourier–Hankel–Gauss transformation of the atomic scattering factor

(1) *Introduction*

It is well known that the isotropic thermal vibrations of an atom in a crystal reduce the f-factor for Bragg reflexions by the Debye–Waller temperature factor $\exp(-Bs^2/4)$, where $B = 8\pi^2\overline{u^2}$ and $\overline{u^2}$ is the mean-square displacement of an atom from its average position. B is always positive and finite even at the absolute zero temperature, although the equations for $B = 0$ will be given as a mathematical limit in spite of the uncertainty principle.

The radial electron density, $\varrho_3(r)$, and its two- and one-dimensional projections, $\varrho_2(r)$ and $\varrho_1(r)$, respectively, are then expressed as the Fourier–Hankel–Gauss transformations of the f-factor:

$$\varrho_3(r) = \int_0^{s_0} 4\pi s^2 f(s) \exp(-\tfrac{1}{4}Bs^2) \cdot \frac{\sin 2\pi rs}{2\pi rs} ds, \quad (9)$$

$$\varrho_2(r) = \int_0^{s_0} 2\pi s f(s) \exp(-\tfrac{1}{4}Bs^2) . J_0(2\pi rs) ds, \quad (10)$$

$$\varrho_1(r) = \int_0^{s_0} 2 f(s) \exp(-\tfrac{1}{4}Bs^2) . \cos(2\pi rs) ds, \quad (11)$$

where $\varrho_3(r) \equiv \varrho(r)$ when $B = 0$ and $J_0(x)$ is the zeroth-order Bessel function of the first kind. Since $f(s)$ is spherically symmetric, $\varrho_3(r)$, $\varrho_2(r)$ and $\varrho_1(r)$ have respectively spherical, circular and linear symmetry with respect to the origin.

The Hankel transformation is self-reciprocal (Erdélyi *et al.*, 1954, vol. 2, p. 3). We have then from equation (10), assuming $s_0 \to \infty$,

$$f(s) \exp(-\tfrac{1}{4}Bs^2) = \int_0^\infty 2\pi r \varrho_2(r) J_0(2\pi sr) dr. \quad (12)$$

Therefore, we may be able to calculate the f-factor from the electron density in the two-dimensional projection. This transformation is valid in all cases, except in case of the TF model of the electron density with $B = 0$.

---

* If $\varrho(r) = kr^n \exp(-cr)$ and $r \neq 0$, then from (1) we have the Laplace equation,

$$\partial^2 f/\partial p^2 + \partial^2 f/\partial c^2 = 0, \quad (3)$$

where $p \equiv 2\pi s$ in $\sin 2\pi sr$. Equations (4) and (5) are solutions of (3).

The curvature of the density function at the origin,

$$\varrho_n''(0) \equiv (\partial^2 \varrho_n(r)/\partial r^2)_{r=0}\,, \tag{13}$$

supplies important information on the accuracy of the electron-density maps (Cruickshank, 1949). Moreover, $\varrho_n''(0)$ has high sensitivity to the thermal factor. If $B \neq 0$,* then

$$\varrho_3''(0) = -\tfrac{16}{3}\pi^3 \int_0^{s_0} s^4 f(s) \exp(-\tfrac{1}{4}Bs^2)ds\,, \tag{15}$$

$$\varrho_2''(0) = -4\pi^3 \int_0^{s_0} s^3 f(s) \exp(-\tfrac{1}{4}Bs^2)ds\,, \tag{16}$$

$$\varrho_1''(0) = -8\pi^2 \int_0^{s_0} s^2 f(s) \exp(-\tfrac{1}{4}Bs^2)ds\,. \tag{17}$$

In these equations, s_0 should be infinite mathematically, but is finite in practice. We shall call the former a *complete transformation* and the latter an *incomplete transformation*. A number of differential equations may be utilized to solve these integrations. Among them, the following forms are of great interest.

Defining $\varrho_3(r) \equiv \varrho_3(b, q)$, where $4b = B$ and $q \equiv 2\pi r$ in $\sin 2\pi sr$, if $r \neq 0$, we have

$$\partial^2 \varrho_3(b, q)/\partial q^2 = \partial \varrho_3(b, q)/\partial b\,. \tag{18}$$

This equation is exactly that for linear heat conduction or a diffusion process in a non-steady state (Margenau & Murphy, 1943, p. 232). The three-dimensional cases are closely related to the one-dimensional ones as follows:

$$\frac{\partial \varrho_1(r)}{\partial r} = -2\pi r \varrho_3(r);\ \varrho_1''(0) = -2\pi \varrho_3(0);\quad -\frac{8\pi}{3}\frac{\partial \varrho_1''(0)}{\partial B} = \varrho_3''(0)\,. \tag{19}$$

In general, $\varrho_n(0)$ and $\varrho_n''(0)$ are related by

$$16\pi^2 \partial \varrho_n(0)/\partial B = n\varrho_n''(0)\,. \tag{20}$$

Equations (18)–(20) are independent of the form of the f-factor and are valid for all possible values of s_0.

Although both complete and incomplete transformations are given for the TF atoms, the following method to estimate the termination-effect of the X-ray Fourier series on $\varrho_n(0)$ and $\varrho_n''(0)$ may sometimes be useful. For $s \geq s_0$, where $s_0 > 1$ in most of the experimental conditions, we may use the Gaussian approximation,

$$f(s) \exp(-\tfrac{1}{4}Bs^2) = G \exp(-gs^2)\,. \tag{21}$$

G and g may be evaluated by a curve-fitting method. This approximation is better for larger B values and for smaller atomic numbers. Using the relation,

$$\int_{s_0}^{\infty} s^{2n} \exp(-gs^2)ds = (-1)^n \frac{\partial^n}{\partial g^n}\int_{s_0}^{\infty} \exp(-gs^2)ds\,, \tag{22}$$

we obtain the following results for the three-dimensional cases:

$$\Delta\varrho_3(0) = \int_{s_0}^{\infty} 4\pi s^2 f(s) \exp(-\tfrac{1}{4}Bs^2)ds = \frac{\pi G}{g}\left\{\sqrt{\left(\frac{\pi}{g}\right)}\operatorname{erf} c(\sqrt{g}.s_0) + 2s_0 \exp(-gs_0^2)\right\}, \tag{23}$$

$$\Delta\varrho_3''(0) = -\frac{2\pi^3 G}{3g^2}\left\{3\sqrt{\left(\frac{\pi}{g}\right)}\operatorname{erfc}(\sqrt{g}.s_0) + 2s_0(2gs_0^2+3)\exp(-gs_0^2)\right\}, \tag{24}$$

where

$$\operatorname{erfc}(x) = \frac{2}{\sqrt{\pi}}\int_x^{\infty} \exp(-t^2)dt = 1-\operatorname{erf}(x)\,, \tag{25}$$

are the error functions. Under the same approximation as in (21), Higgs (1953) has obtained the equations corresponding to (23) and (24). However, his equations contain an incomplete gamma function and the present results may be more convenient for computation.

The two-dimensional cases are

$$\Delta\varrho_2(0) = \int_{s_0}^{\infty} 2\pi s f(s) \exp(-\tfrac{1}{4}Bs^2)ds = \frac{\pi G}{g}\exp(-gs_0^2)\,, \tag{26}$$

$$\Delta\varrho_2''(0) = -\frac{4\pi^3 G}{g^2}(gs_0^2+1)\exp(-gs_0^2)\,. \tag{27}$$

The one-dimensional ones, if necessary, can be readily obtained from (19), (22) and (23).

(2) *Hydrogen atom*

The results given in this section are applicable to the 1s electron of any atom or to the density distribution with $n = 0$ in equation (2). Expressions for $\varrho_3(r)$ and $\varrho_2(0)$ are omitted, since they are given by McDonald (1956).

Using the dimensionless quantities, $\gamma = B/(4\pi^2 a_0^2)$ and $R = r/a_0$, where a_0 is the Bohr radius, we have

$$\varrho_2(r) = \frac{2\exp(\gamma)}{\pi a_0^2}\{R\varkappa_1(2R, \gamma) - \gamma\varkappa_0(2R, \gamma)\}\,, \tag{28}$$

$$\varrho_1(r) = \frac{\exp(\gamma)}{4a_0}\left\{(1+2R-2\gamma)\exp(-2R).\operatorname{erfc}\left(\sqrt{\gamma}-\frac{R}{\sqrt{\gamma}}\right) + (1-2R-2\gamma)\exp(2R).\operatorname{erfc}\left(\sqrt{\gamma}+\frac{R}{\sqrt{\gamma}}\right) + 4\sqrt{\left(\frac{\gamma}{\pi}\right)}\exp\left(-\frac{R^2}{\gamma}-\gamma\right)\right\}, \tag{29}$$

where $\varkappa_0(2R, \gamma)$ and $\varkappa_1(2R, \gamma)$ are the incomplete

---

* In equations (15)–(17), we employ

$$\lim_{r\to 0}\frac{\partial^2}{\partial r^2}\int_0^{s_0} \exists(s, B, r)ds = \int_0^{s_0}\lim_{r\to 0}\frac{\partial^2}{\partial r^2}\exists(s, B, r)ds\,. \tag{14}$$

By Lebesque's convergence theorem (Saks, 1937, p. 114) and its extension, (14) is generally true if $B \neq 0$, and in a few cases this is valid even if $B = 0$. Use of (14) avoids difficult computations.

modified Hankel function of order zero and one, respectively (cf. Appendix). Noting that $\gamma < 1$ when $B < 11{\cdot}1$ Å^2, we have the following results from equation (28):

$$\varrho_2(r) = \frac{\exp(\gamma)}{\pi a_0^2}\left\{2RK_1(2R) - 2\gamma K_0(2R) - \gamma Ei\left(-\frac{R^2}{\gamma}\right) + \sum_{n=1}^{\infty}\frac{(-1)^n}{n!}(\gamma+n)R^{2n}\int_{R^2/\gamma}^{\infty}\frac{\exp(-t)}{t^{n+1}}dt\right\}, \quad (30)$$

where $K_0(2R)$ and $K_1(2R)$ are the modified Hankel functions (Watson, 1952, p. 698). The integral in (30) can be evaluated by using the exponential integral,

$$-Ei(-x) = \int_x^{\infty}\frac{\exp(-t)}{t}dt, \quad (31)$$

and the recursion formula,

$$\int_x^{\infty}\frac{\exp(-t)}{t^{n+1}}dt = \frac{1}{n}\left(\frac{\exp(-x)}{x^n} - \int_x^{\infty}\frac{\exp(-t)}{t^n}dt\right). \quad (32)$$

Only a few terms are required here, because (32) converges rapidly with n.

If $R > 1$ ($r > 0{\cdot}5291$ Å), by using the asymptotic expansion of the error function, $\varrho_3(r)$ and $\varrho_1(r)$ may be approximated by

$$\varrho_3(r) \cong \frac{1}{\pi a_0^3}\left(1-\frac{\gamma}{R}\right)\exp(\gamma-2R), \quad (33)$$

$$\varrho_1(r) \cong \frac{1}{2a_0}(1+2R-2\gamma)\exp(\gamma-2R). \quad (34)$$

Similar approximation formulae may be obtained readily for any of the equations given in the present paper.

If $r = 0$ and $B \neq 0$, we have (cf. Appendix)

$$\varrho_3(0) = \frac{1}{\pi a_0^3}\left\{(1+2\gamma)\exp(\gamma).\mathrm{erfc}(\sqrt{\gamma}) - 2\sqrt{\left(\frac{\gamma}{\pi}\right)}\right\}, \quad (35)$$

$$\varrho_1(0) = \frac{1}{2a_0}\left\{(1-2\gamma)\exp(\gamma).\mathrm{erfc}(\sqrt{\gamma}) + 2\sqrt{\left(\frac{\gamma}{\pi}\right)}\right\}. \quad (36)$$

The curvatures for $r = 0$ and $B \neq 0$ are

$$\varrho_3''(0) = -\frac{4}{3\pi a_0^5}\left\{-(3+2\gamma)\exp(\gamma).\mathrm{erfc}(\sqrt{\gamma}) + 2 \times \sqrt{\left(\frac{\gamma}{\pi}\right)}\left(\frac{1}{\gamma}+1\right)\right\}, \quad (37)$$

$$\varrho_2''(0) = \frac{2}{\pi a_0^4}\{(1+\gamma)\exp(\gamma).Ei(-\gamma)+1\}. \quad (38)$$

$\varrho_1''(0)$ can be obtained from (19) and (35).

(3) *Many-electron atom*

The three- and two-dimensional cases are given in this section. For $\varrho(r) = kr^n\exp(-cr)$, using the dimensionless parameters, $\eta = Bc^2/(16\pi^2)$ and $R = cr/2$, we have

$$\varrho_3(r) = \frac{(n+1)!\,2^{n/2-1}k\eta^{(n+1)/2}}{\sqrt{\pi}.c^nR}\exp\left(-\frac{R^2}{\eta}\right) \times\left[\exp\left\{\frac{\eta}{2}\left(1-\frac{R}{\eta}\right)^2\right\}\cdot D_{-(n+2)}\left\{\sqrt{(2\eta)}\left(1-\frac{R}{\eta}\right)\right\} - \exp\left\{\frac{\eta}{2}\left(1+\frac{R}{\eta}\right)^2\right\}\cdot D_{-(n+2)}\left\{\sqrt{(2\eta)}\left(1+\frac{R}{\eta}\right)\right\}\right], \quad (39)$$

where $D_{-\nu}(x)$ is the parabolic cylinder function.

For the two-dimensional case, we have the following general solution for our integral:

$$\int_0^{\infty}\frac{s\exp(-\frac{1}{4}Bs^2)}{(s^2+c^2/4\pi^2)^{n+1}}J_0(2\pi rs)ds = \frac{B^n}{2^{2n}n!} \times\exp(\eta)\sum_{m=0}^{n}\left\{(-1)^m\binom{n}{m}\left(\frac{R}{\eta}\right)^{n-m}\varkappa_{n-m}(2R,\eta)\right\}. \quad (40)$$

The cases for $r = 0$, $B \neq 0$ and $0 < n < 3$ are as follows:

(i) $\varrho(r) = kr\exp(-cr)$:

$$\varrho_3(0) = \frac{2k}{c}\left\{-\eta(2\eta+3) \times\exp(\eta).\mathrm{erfc}(\sqrt{\eta}) + 2\sqrt{\left(\frac{\eta}{\pi}\right)}(\eta+1)\right\}, \quad (41)$$

$$\varrho_2(0) = \frac{2k}{c^2}\{-\eta(2\eta+1)\exp(\eta).Ei(-\eta) - 2\eta + 1\}. \quad (42)$$

(ii) $\varrho(r) = kr^2\exp(-cr)$:

$$\varrho_3(0) = \frac{2k\eta}{c^2}\left\{(4\eta^2+12\eta+3) \times\exp(\eta).\mathrm{erfc}(\sqrt{\eta}) - 2\sqrt{\left(\frac{\eta}{\pi}\right)}(2\eta+5)\right\}, \quad (43)$$

$$\varrho_2(0) = \frac{4k}{c^3}\{\eta^2(2\eta+3)\exp(\eta).Ei(-\eta) + 2\eta^2+\eta+1\}. \quad (44)$$

The expressions for $\varrho_3''(0)$ and $\varrho_2''(0)$ for $0 < n < 3$ are:

(i) $\varrho(r) = kr\exp(-cr)$:

$$\varrho_3''(0) = -\tfrac{2}{3}kc\left\{(2\eta^2+7\eta+3) \times\exp(\eta).\mathrm{erfc}(\sqrt{\eta}) - 2\sqrt{\left(\frac{\eta}{\pi}\right)}\left(\eta+3+\frac{1}{2\eta}\right)\right\}, \quad (45)$$

$$\varrho_2''(0) = -k\{(2\eta^2+5\eta+1)\exp(\eta).Ei(-\eta) + 2\eta + 3\}. \quad (46)$$

(ii) $\varrho(r) = kr^2\exp(-cr)$:

$$\varrho_3''(0) = -\frac{2k}{3}\left\{-(4\eta^3+24\eta^2+27\eta+3)\exp(\eta).\mathrm{erfc}(\sqrt{\eta}) + 2\sqrt{\left(\frac{\eta}{\pi}\right)}(2\eta^2+11\eta+9)\right\}, \quad (47)$$

$$\varrho_2''(0) = \frac{2k}{c}\{(2\eta^2+9\eta+6)\eta \times\exp(\eta).Ei(-\eta) + 2\eta^2+7\eta+1\}. \quad (48)$$

(4) *The Thomas–Fermi atom*

(*a*) *The complete transformation.*—Denoting $4P_n = B\beta_n Z^{2/3}$ and $Q_n = \pi\sqrt{\beta_n}.Z^{1/3}r$, where dimensionally $[P_n] \equiv [Q_n] \equiv 0$, we have

$$\varrho_3(r) = \frac{\pi^2 Z^2}{2} \sum_n \frac{\alpha_n \beta_n^{3/2}}{Q_n} \exp(P_n) \times \left\{ \exp(-2Q_n).\operatorname{erfc}\left(\sqrt{P_n} - \frac{Q_n}{\sqrt{P_n}}\right) - \exp(2Q_n).\operatorname{erfc}\left(\sqrt{P_n} + \frac{Q_n}{\sqrt{P_n}}\right)\right\}, \quad (49)$$

$$\varrho_2(r) = 2\pi Z^{5/3} \sum_n \alpha_n \beta_n \exp(P_n).\varkappa_0(2Q_n, P_n), \quad (50)$$

$$\varrho_1(r) = \frac{\pi Z^{4/3}}{2} \sum_n \alpha_n \sqrt{\beta_n} \exp(P_n) \times \left\{ \exp(-2Q_n).\operatorname{erfc}\left(\sqrt{P_n} - \frac{Q_n}{\sqrt{P_n}}\right) + \exp(2Q_n).\operatorname{erfc}\left(\sqrt{P_n} + \frac{Q_n}{\sqrt{P_n}}\right)\right\}, \quad (51)$$

where the limit on n is 3, corresponding to the Rozental three-term approximation. Note that $Q_n/\sqrt{P_n}$ is equal to $2\pi r/\sqrt{B}$ and is independent of n.

When $r = 0$ but $B \neq 0$, the results are

$$\varrho_3(0) = 2\pi Z^2 \sum_n \alpha_n \beta_n^{3/2} \{\sqrt{(\pi/P_n)} - \pi \times \exp(P_n).\operatorname{erfc}(\sqrt{P_n})\}, \quad (52)$$

$$\varrho_2(0) = \pi Z^{5/3} \sum_n \alpha_n \beta_n \exp(P_n).\{-Ei(-P_n)\}, \quad (53)$$

$$\varrho_1(0) = \pi Z^{4/3} \sum_n \alpha_n \sqrt{\beta_n} \exp(P_n).\operatorname{erfc}(\sqrt{P_n}). \quad (54)$$

The following equations for $r \neq 0$ and $B = 0$ will give the standard peak shape of a TF atom at rest:

$$\varrho_3(r) = \pi^2 Z^2 \sum_n \frac{\alpha_n \beta_n^{3/2}}{Q_n} \exp(-2Q_n), \quad (55)$$

$$\varrho_2(r) = 2\pi Z^{5/3} \sum_n \alpha_n \beta_n K_0(2Q_n), \quad (56)$$

$$\varrho_1(r) = \pi Z^{4/3} \sum_n \alpha_n \sqrt{\beta_n} \exp(-2Q_n). \quad (57)$$

When both $r = 0$ and $B = 0$, the peak heights in the three- and two-dimensional cases become infinite, but $\varrho_1(0) = 1{\cdot}417 Z^{4/3}$. However, it can be proved that

$$\int_0^\infty 4\pi r^2 \varrho_3(r)\, dr = \int_0^\infty 2\pi r \varrho_2(r)\, dr = Z, \quad (58)$$

and the physical interpretation is still valid as in other cases.

The curvatures for $r = 0$ and $B \neq 0$ are as follows:

$$\varrho_3''(0) = -\tfrac{1}{3}\pi^2 Z^{8/3} \sum_n \alpha_n \beta_n^{5/3} \left(\frac{\pi}{P_n}\right)^{3/2} \times [1 - 2P_n\{1 - \sqrt{(\pi P_n)} \exp(P_n).\operatorname{erfc}(\sqrt{P_n})\}], \quad (59)$$

$$\varrho_2''(0) = -2\pi^3 Z^{7/3} \sum_n \alpha_n \beta_n^2 \times \left\{\frac{1}{P_n} + \exp(P_n).Ei(-P_n)\right\}. \quad (60)$$

(*b*) *The incomplete transformation.*—As may be expected, mathematical complexity increases in the incomplete transformation. Various types of series expansion can be utilized for the general cases. However, these cases require unnecessarily lengthy explanation. Consequently, only those cases which are of immediate interest to us are discussed here.

In the case, $r = 0$ and $B \neq 0$, by introducing again the dimensionless variables, $S_0 = s_0\sqrt{B}/2$ and $q_n = \sqrt{\beta_n}.Z^{1/3}/s_0$, where $P_n = S_0^2 q_n^2$, we have

$$\varrho_3(0) = 2\pi Z^2 \sum_n \alpha_n \beta_n^{3/2} \left[\sqrt{\left(\frac{\pi}{P_n}\right)} \operatorname{erf}(S_0) - 2\exp(P_n)\left\{\arctan\frac{1}{q_n} - 2q_n W(S_0, q_n)\right\}\right], \quad (61)$$

$$\varrho_2(0) = \pi Z^{5/3} \sum_n \alpha_n \beta_n \times \exp(P_n)[Ei\{-(S_0^2 + P_n)\} - Ei(-P_n)], \quad (62)$$

$$\varrho_1(0) = 2Z^{4/3} \sum_n \alpha_n \sqrt{\beta_n} \times \exp(P_n)\left\{\arctan\frac{1}{q_n} - 2q_n W(S_0, q_n)\right\}, \quad (63)$$

where

$$W(S_0, q_n) = \int_0^{S_0} \exp(-q_n^2 y^2) \int_0^y \exp(-x^2)\, dx\, dy. \quad (64)$$

This double integral has been investigated extensively by Rosser (1948).

When both $r = 0$ and $B = 0$, we have

$$\varrho_3(0) = 4\pi Z^2 \sum_n \alpha_n \beta_n^{3/2} \left(\frac{1}{q_n} - \arctan\frac{1}{q_n}\right), \quad (65)$$

$$\varrho_2(0) = \pi Z^{5/3} \sum_n \alpha_n \beta_n \ln\left(1 + \frac{1}{q_n^2}\right), \quad (66)$$

$$\varrho_1(0) = 2Z^{4/3} \sum_n \alpha_n \sqrt{\beta_n} \arctan\frac{1}{q_n}, \quad (67)$$

where equations (65)–(67) are functions of $s_0 Z^{-1/3}$ alone.

When $r = 0$ but $B \neq 0$, the curvatures are

$$\varrho_3''(0) = -\tfrac{8}{3}\pi^3 Z^{8/3} \sum_n \frac{\alpha_n \beta_n^{5/2}}{P_n} \left[(\tfrac{1}{2} - P_n)\sqrt{\left(\frac{\pi}{P_n}\right)} \times \operatorname{erf}(S_0) - \frac{1}{q_n}\exp(-S_0^2) + 2P_n \times \exp(P_n)\left\{\arctan\frac{1}{q_n} - 2q_n W(S_0, q_n)\right\}\right], \quad (68)$$

$$\varrho_2''(0) = -2\pi^3 Z^{7/3} \sum_n \frac{\alpha_n \beta_n^2}{P_n} [1 - \exp(-S_0^2) - P_n \exp(P_n) \times \{Ei(-S_0^2 - P_n) - Ei(-P_n)\}]. \quad (69)$$

The curvatures for both $r = 0$ and $B = 0$ are functions of $s_0 Z^{-1/3}$ alone.

$$\varrho_3''(0) = -\tfrac{16}{9}\pi^3 Z^{8/3} \sum_n \alpha_n \beta_n^{5/2} \left(\frac{1}{q_n^3} - \frac{3}{q_n} + \frac{3}{q_n^{3/2}} \arctan \frac{1}{q_n} \right), \tag{70}$$

$$\varrho_2''(0) = -2\pi^3 Z^{7/3} \sum_n \alpha_n \beta_n^2 \left\{ \frac{1}{q_n^2} - \ln\left(\frac{1}{q_n^2} + 1 \right) \right\}. \tag{71}$$

4. Application

Since extensive tables such as those published by the National Bureau of Standards or highly convergent series are available for all of the transcendental functions used in this paper, and since all equations introduced are closely related to each other, the numerical evaluations can be carried out without much difficulty.

The one-dimensional case has not been used very often in structure analyses. However, it is closely related to the three-dimensional case as in (19), and furthermore it is useful in interpreting other higher-dimensional cases in our transformations, as discussed below.

(1) *Hydrogen atom*

As discussed later in detail, the peak density of lighter atoms is mostly due to the 1*s* electron when B is small. Therefore, the results for the hydrogen atom will have considerable generality. The peak density, $\varrho_n(0)$, and the peak curvature, $\varrho_n''(0)$, of hydrogen atom are shown in Fig. 1, as a function of B. It is readily seen that the dependency of the peak curvature on B is much greater than that of the peak density. This is generally true for all atoms over a wide range of B.

For both $\varrho_n(0)$ and $\varrho_n''(0)$, the three-dimensional case ($n = 3$) initially gives exponentially decreasing curves, and the one-dimensional case ($n = 1$) is relatively insensitive to B, while the two-dimensional case ($n = 2$) lies more or less between these two cases. One notes that there are critical values of B, beyond which the $n = 3$ case will no longer have larger values of $\varrho_n(0)$ or $\varrho_n''(0)$ than those in other cases. This fact may be very instructive in locating the hydrogen position, since the accuracy of the atomic co-ordinates in the electron-density maps increases as the peak curvature increases (Cruickshank, 1949). Furthermore, the Fourier ripple-effect of a heavier atom near the hydrogen would be decreased relatively as the hydrogen peak-density increases. Accordingly, if the B-value is greater than all of these critical values ($B > 5{\cdot}3$ Å^2, i.e. $(\overline{u^2})^{\frac{1}{2}} > 0{\cdot}26$ Å), use of the three-dimensional synthesis will no longer increase the accuracy of the hydrogen co-ordinates in the X-ray Fourier methods. However, the three-dimensional synthesis has greater advantage in resolving the peaks. Although all atoms have critical B values, the above discussion becomes less important in heavier atoms. This is because their critical B values for the peak densities are usually considerably large (Fig. 5) and those for the peak curvatures are always much greater than those for the peak densities.

(2) *Many-electron atom*

All numerical results given in Figs. 2–4 are based on the Duncanson–Coulson wave functions (1944). From these figures, one can readily find the peak

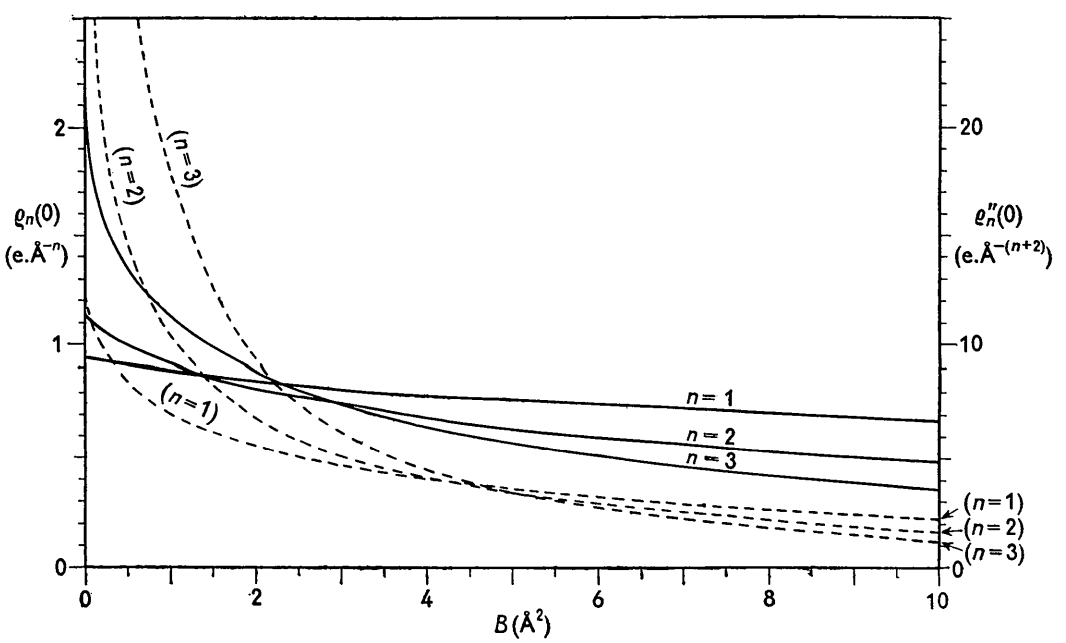

Fig. 1. Hydrogen atom: the peak density, $\varrho_n(0)$ in solid lines, and the peak curvature, $\varrho_n''(0)$ in broken lines, as a function of B.

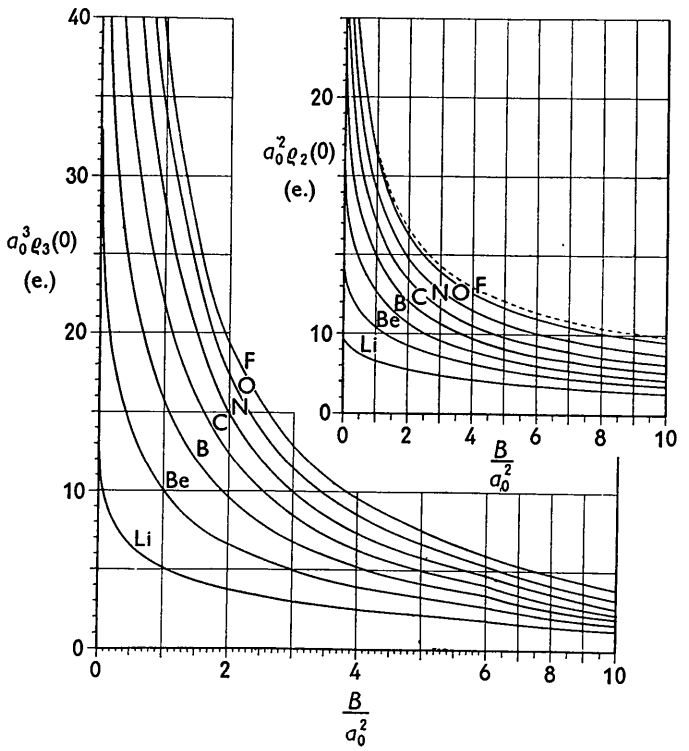

Fig. 2. The peak densities of atoms in their ground states from lithium to fluorine in the three- and two-dimensional cases of the complete transformations, where $0 \leq B < 2{\cdot}8$ Å^2. The peak density of the fluorine ion in the two-dimensional case is also shown by the broken line. The other possible valence or ionic states are not shown here, because they are not clearly distinguishable from the curves shown. All values are measured in the atomic unit.

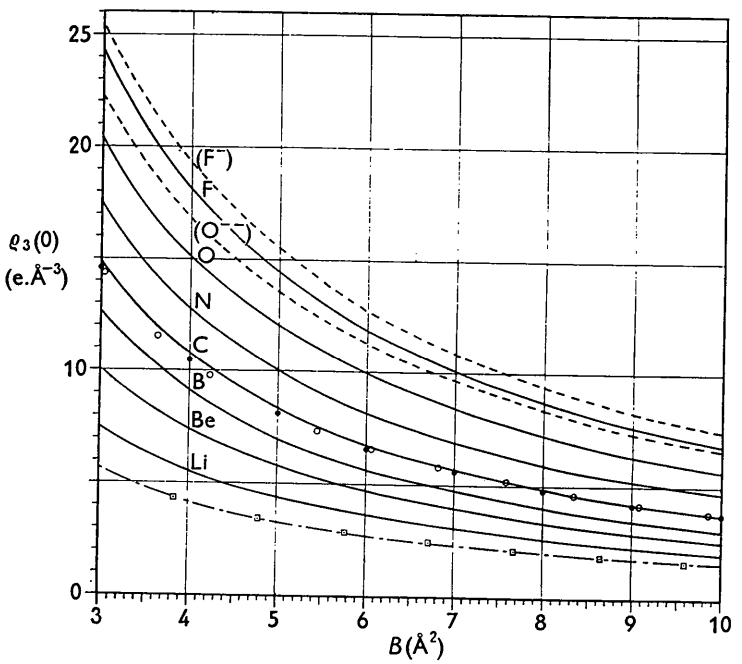

Fig. 3. The peak densities of atoms lithium to fluorine in the three-dimensional case of the complete transformations, where 3 Å$^2 \leq B \leq 10$ Å^2. The results obtained from the Duncanson–Coulson wave functions are shown by solid lines for the ground states, by broken lines for the ionic states, and by filled circles for sp^3 carbon atom. The values for the TF carbon and lithium atoms are shown by open circles and squares, respectively.

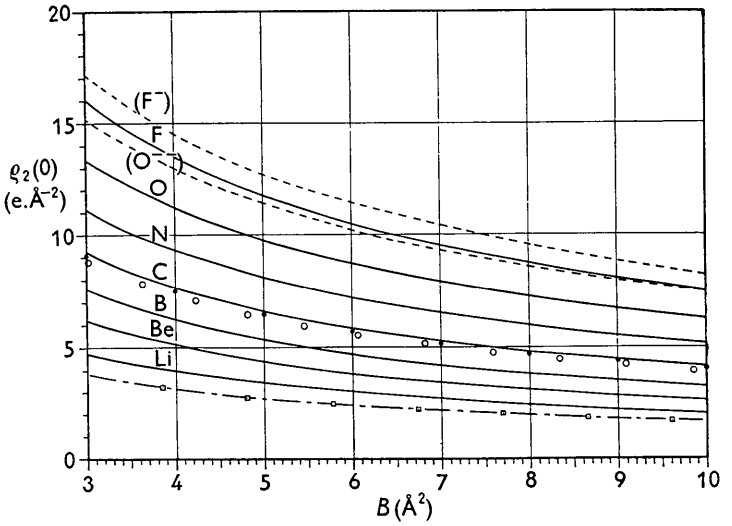

Fig. 4. The two-dimensional case using the same notation as in Fig. 3.

Table 1. *Comparison between observed and calculated values of* $\varrho_n(0)$ *and* $\varrho_n''(0)$, *where* $n = 2$ *or* 3.

Values of $\varrho_n(0)$ in e.Å^{-n}; values of $\varrho_n''(0)$ in e.Å$^{-(n+2)}$

Atom (n) Crystal	Cl(2) B_2Cl_4*	Cl(2) B_4Cl_4†	C(3) 1,8-Diphenyl-1,3,5,7-octatetraene‡	C(3) Oxamid§	N(3) Oxamid§	O(3) Oxamid§	F(3) SiF_4//	Si(3) SiF_4//
B (Å^2)	1·6	3·5	1·93	1·698	2·055	2·055	4·1	4·1
s_0 (Å^{-1})	1·321	1·321	1·297	2·16	2·16	2·16	1·268	1·268
$\langle\varrho_n(0)_{obs.}\rangle_{av.}$	34	24	10·4	17·5	17·9	20·0	12	23
$\langle\varrho_n''(0)_{obs.}\rangle_{av.}$	421	242	105	321	303	316	96	169
			Complete transformation					
$\varrho_n(0)_{calc.}$ (i)	—	—	23·6	27·2	25·4	29·2	16·8	—
$\varrho_n(0)_{calc.}$ (ii)	48·4	28·7	22·4	25·6	25·6	30·5	16·7	29·0
$\varrho_n''(0)_{calc.}$ (i)	—	—	725	939	728	801	216	—
$\varrho_n''(0)_{calc.}$ (ii)	1535	451	637	819	692	828	239	423
			Incomplete transformation					
$\varrho_n(0)_{calc.}$ (*a*)	33·8	25·4	11·3	22·8	22·8	26·5	13·1	24·5
$\varrho_n(0)_{calc.}$ (*b*)	33·2	25·2	11·9	22·0	23·2	27·6	12·9	22·5
$\varrho_n(0)_{calc.}$ (*c*)	—	—	11·4	22·9	22·5	26·0	—	—
$\varrho_n''(0)_{calc.}$ (*a*)	437	270	117	543	489	544	107	182
$\varrho_n''(0)_{calc.}$ (*b*)	415	264	123	491	477	562	113	198
$\varrho_n''(0)_{calc.}$ (*c*)	—	—	120	552	478	518	—	—
$\frac{\varrho_n(0)_{obs.}}{\varrho_n(0)_{calc.}\ (a)}$	1·0	0·94	0·92	0·77	0·79	0·75	0·92	0·94
$\frac{\varrho_n''(0)_{obs.}}{\varrho_n''(0)_{calc.}\ (a)}$	0·96	0·90	0·90	0·59	0·62	0·58	0·90	0·93

(i) From the electronic wave functions for the ground state.
(ii) Thomas–Fermi–Rozental method.
(*a*) Graphical integration using $f(s)$ given by Berghuis *et al.* (1955) or given in the *International Tables* (1935).
(*b*) Thomas–Fermi–Rozental incomplete transformation.
(*c*) The results using the Gaussian approximation of equations (23) and (24), in which $G = 1{\cdot}754$ e., $g = 0{\cdot}113$ Å$^2 + \frac{1}{4}B$ for carbon; $G = 1{\cdot}76$ e., $g = 0{\cdot}0811$ Å$^2 + \frac{1}{4}B$ for nitrogen; $G = 1{\cdot}79$ e., $g = 0{\cdot}0658$ Å$^2 + \frac{1}{4}B$ for oxygen.

* Atoji, Lipscomb & Wheatley (1955).
† Atoji & Lipscomb (1953).
‡ Drenth & Wiebenga (1955).
§ Ayerst & Duke (1954).
// Atoji & Lipscomb (1954).

heights of the atoms in the first row of the periodic table, except neon, as a function of B. Since these values are obtained from the complete transformations, they will give the maximum possible values of the peak heights. The peak curvatures can be obtained from these figures and equation (20), or directly from equations (37), (38) and (45)–(48). The series-termination effect may be evaluated by using the Gaussian approximation as in equations (21)–(27), or by the graphical integration of the original expression using the best scattering factor (cf. Table 1).

It is found in all atoms that the $2s$-electron densities at the origin are less sensitive to B than those of the $1s$ electron, although both decrease similarly with increasing B. The $2p$-electron density at the origin in the three-dimensional case is zero when the atom is at rest. As the mean amplitude of vibrations of the atom increases, the number of the $2p$ electrons found at the origin first increases rather sharply and then decreases very gradually. On the other hand, the two-dimensional case is finite at the origin when the atom is at rest, and is very insensitive to changes in the thermal factor.

Although the contributions of the $2s$ and $2p$ electrons to the peak densities of the atoms are small for small values of B, these become relatively important as B increases, because of their different dependencies on the temperature factor. In addition, these contributions are rather greater in the two-dimensional case than in three dimensions. For example, in the ground state of the fluorine atom, the $2p$ contributions to $\varrho_3(0)(\varrho_2(0))$ are 24% (35%) at $B = 3$ Å^2 and 40% (45%) at $B = 8$ Å^2.

In the extended Figs. 3 and 4, the peak densities of the iso-electronic atoms $O^=$ and F^- are shown. The difference between these two atoms is statistically significant even with the present accuracy of X-ray methods, because the standard deviation of the electron density in the Fourier maps is less than 0·4 e.Å^{-n} in most of the reported structures (cf. Cruickshank, 1949). It may also be noted that the difference between the peak densities of $O^=$ and F^- is almost invariant with respect to the temperature factor.

The differences between the ground and valence states in any atom are very small in the peak values, as seen from the case of the carbon atom in Figs. 3 and 4. Consequently, for distinguishing the different valence states, the non-spherical nature or the directional property of the bonding electron distribution may be more useful than the peak value. The density distribution of the electrons having non-spherical symmetry, such as the $2p$ electrons, may be evaluated from (39) and (40) for the special spherical angles (cf. Higgs, 1953).

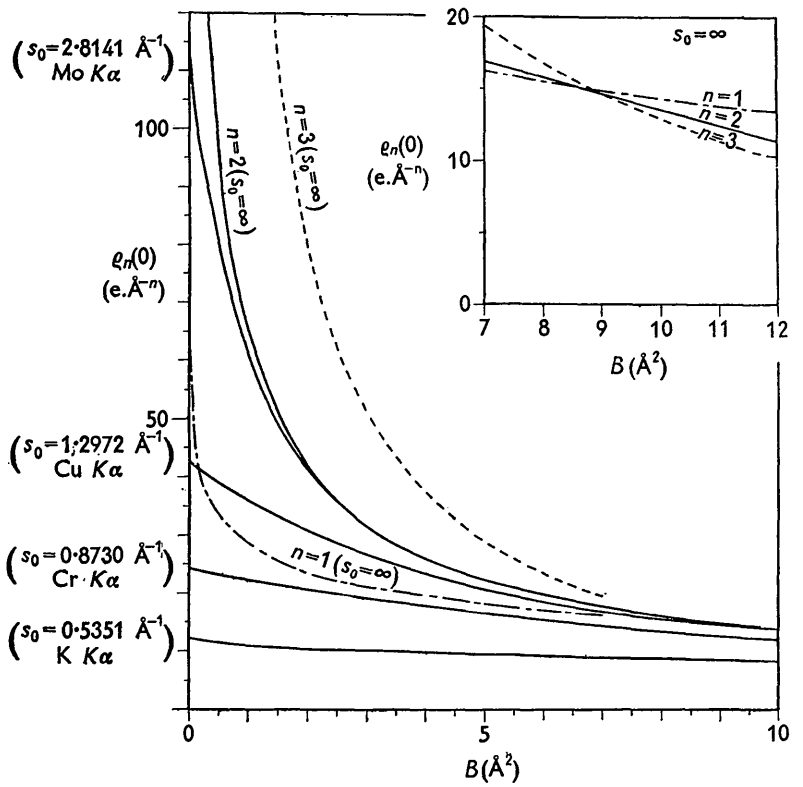

Fig. 5. The peak density of the TF chlorine atom in the two-dimensional complete and incomplete transformations as a function of B. The three- and one-dimensional complete transformations are also shown by broken lines. The critical B values may be seen from the inserted figure at the upper right corner.

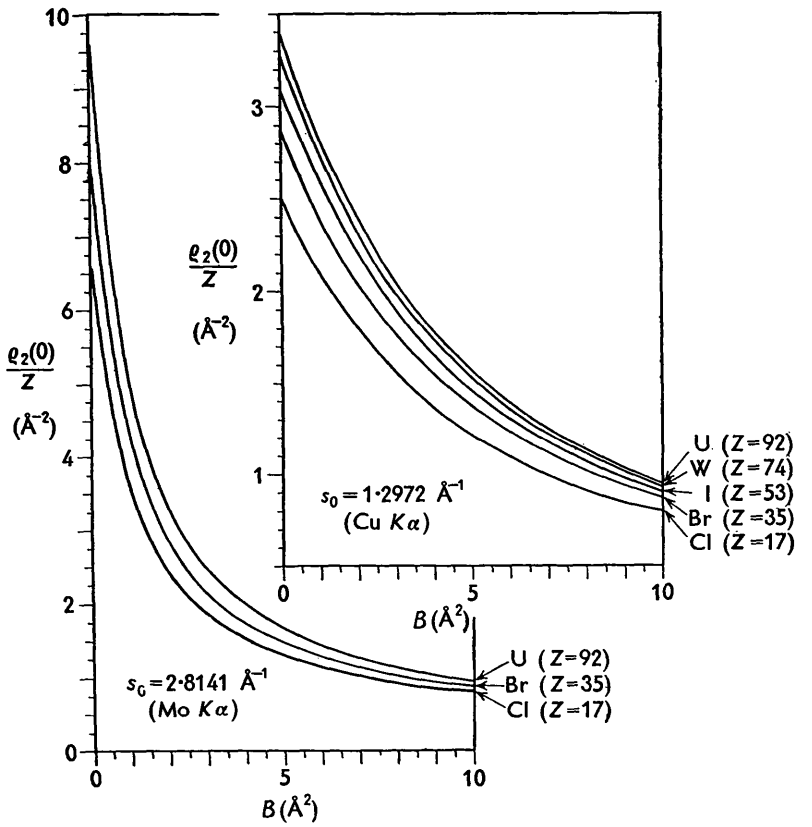

Fig. 6. The peak densities per nuclear charge of the TF atoms for various B values in the two-dimensional incomplete transformations under two experimental conditions.

We now know the dependency of the density distribution on B of each electronic orbital. If very precise X-ray data at different temperatures were available, the quantitative analysis of the electron distributions in Fourier maps of various dimensions would give useful information to molecular theories and to the re-determination of the screening constants in wave functions.

(3) *The Thomas–Fermi atom*

All numerical results given for the TF atoms are based on the Rozental three-term approximation.

As is well known, the f-factor of the TF atom is a function of $sZ^{\frac{1}{3}}$ alone (cf. equation (6)). Correspondingly, $\varrho_n(r)/Z^{n/3+1}$ of the TF atom is a function of two variables, $Z^{\frac{1}{3}}/B$ and $Z^{\frac{1}{3}}r$. Therefore, the results for the complete transformations given in Figs. 5–8 can be easily converted to any other TF atom. On the other hand, for the incomplete transformation, two more variables, $\sqrt{B}.s_0$ and $Z^{-\frac{1}{3}}s_0$, are required. Accordingly, the conversion in the incomplete transformation always accompanies the change of both experimental parameters, B and s_0. Therefore, except in very special cases, the simple generality such as in the conversion of the f-factors may not be found in the incomplete transformation.

When smaller values of s_0 are taken for the limit of the observation, the decreasing sensitivity to the B-value is reflected in the peak value. This is generally true for all atoms, and for both the wave functions and the TF methods. An example is shown in Fig. 5, from which one may see that the peak values are almost invariant with respect to B when a long-wavelength radiation is used.

In any case, the difference between $\varrho_n(0)$'s or $\varrho_n''(0)$'s decrease as B increases. For instance, if $B > 2{\cdot}5$ Å^2, the peak values for Mo $K\alpha$ ($s_0 = 2{\cdot}8141$ Å^{-1}) are well approximated by ones for $s_0 = \infty$ in any TF atom in the two-dimensional case (Fig. 5).

The values, $\varrho_2(0)/(\varrho_2(0))_{B=0}$ for a wide range of B, are almost the same for the TF atoms with $Z \geq 17$ for any s_0 value. This may be seen from Fig. 6, from which one also can obtain the peak values of the TF atoms in the two-dimensional projection for Mo $K\alpha$ and Cu $K\alpha$.

It is also found that there are critical s_0 values. If s_0 is less than these critical values, the relation, $\varrho_3(0) > \varrho_2(0) > \varrho_1(0)$ changes reciprocally to $\varrho_3(0) < \varrho_2(0) < \varrho_1(0)$. A similar relation is shown for the peak curvature. In other words, the peak values in various dimensions for $s_0 < s_0$(critical) show similar behavior to that for $B > B$(critical) (Figs. 1 and 7).

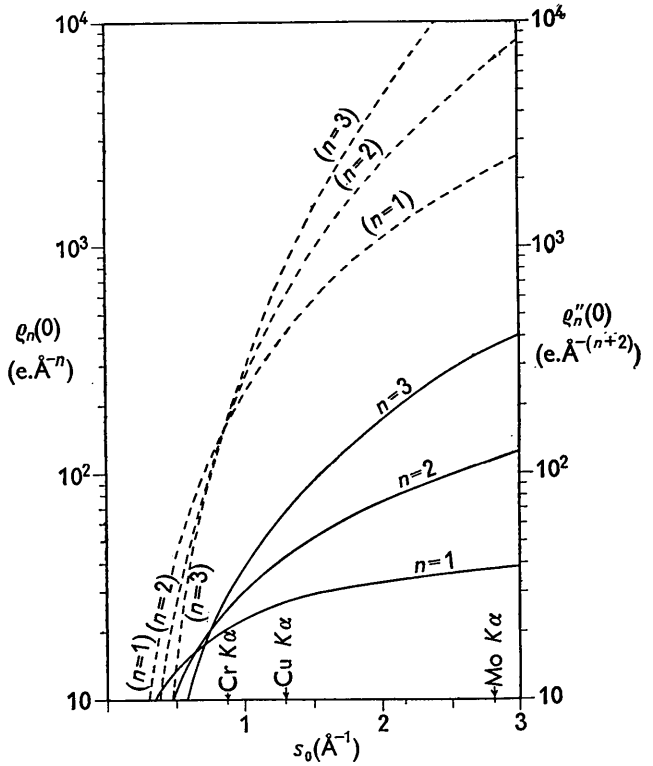

Fig. 7. The series-termination effect on both peak density and the peak curvature of the TF chlorine atom with $B = 0$; $\varrho_n(0)$ in solid lines and $\varrho_n''(0)$ in broken lines. The ordinate is in logarithmic scale.

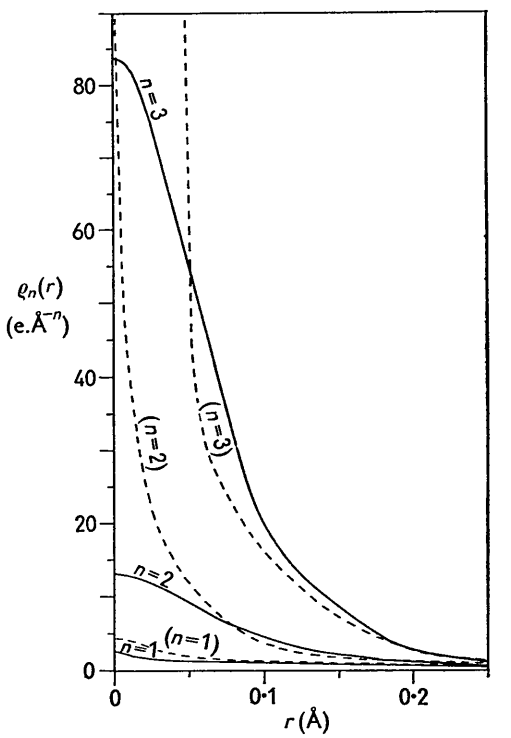

Fig. 8. The effect of the zero-point vibrations on the electron distribution of the TF copper atom in the complete transformations. The physical limiting case ($B = 0{\cdot}14$ Å^2) is shown by solid lines, and the mathematical limiting case ($B = 0$) by broken lines.

The existence of a critical s_0 should be realized in the preliminary stages of X-ray Fourier analysis, where one often uses the data within a small $\sin\theta/\lambda$ range.

The TF statistical approximation is less reliable for the lighter atoms, as seen in the case of the lithium atom in Figs. 3 and 4. However, in general, the TF model for these lighter atoms becomes more satisfactory as B increases. This may be because the electronic orbitals of the atom are smoothed out by the thermal vibrations, and the statistical treatment of charge distribution becomes suitable even for these lighter atoms. In Figs. 3 and 4, one may notice that even the carbon atom, which has only six electrons, may be treated by the TF method, provided that the thermal motion of the atom is appreciably large. In the case of the fluorine atom, the difference between the results obtained by the electronic wave functions and by the TF method is negligible for $B > 3$ Å^2.

(4) *Comparison with experiment*

The peak density and the peak curvature calculated from the wave functions and the TF method are compared with the observed data in the two- and three-dimensional cases in Table 1. As indicated by the ratio between the observed and calculated values, the observed peak values are always smaller than the calculated ones. This is because the very weak reflections are not used in the Fourier synthesis of the electron-density maps. Moreover, these weak reflections are usually more frequently observed at larger s-values. Therefore, the effect of these rejected reflections is greater in the peak curvature than in the peak density as realized from the integrands in equations (9)–(17). This can be seen particularly from the results for oxamid crystals. The unreliability of the intensity measurement of the X-ray reflection at small $\sin\theta/\lambda$ does not affect greatly the peak values. The graphical integrations were done with a polar planimeter, using equations (9), (10), (22) and (23) along with the best $f(s)$ available.

(5) *Other possible applications*

B consists of two parts, B_0 and B_T, where B_T depends on the temperature T and B_0 is independent of the temperature, having its origin in the zero-point energy of the crystal lattice. Therefore $\lim_{T\to 0} B = B_0$ and

$$B_0 = \frac{3}{2}\frac{h^2}{m_A k\Theta} \quad \text{and} \quad B_T = \frac{6h^2T}{m_A k\Theta}\,\vartheta\left(\frac{\Theta}{T}\right), \qquad (72)$$

where m_A is the atomic mass, h and k are respectively Planck's and Boltzmann's constant, Θ is the characteristic temperature of the crystal and $\vartheta(x)$ is tabulated

as a function of x (James, 1950, p. 219). The effect of B_0 on the f-factor is by no means negligible at large values of $\sin\theta/\lambda$. Correspondingly, B_0 may considerably modify the peak-shape at small values of r. This is most strikingly demonstrated by the TF copper atom at 0° K. in Fig. 8, where $\Theta = 320°$ K. and $B_0 = 0{\cdot}14$ Å^2 (James, 1950, p. 221).

If the electron distributions of the atoms in a crystal at various temperatures are determined accurately with Fourier maps, such as in the case of *α-trans*-cinnamic acid (Ladell, McDonald & Schmidt, 1956), the characteristic temperature may be determined, at least approximately, from equation (72) and others given in this paper.

In the difference synthesis for the refinement of the temperature factors of atoms, if atomic co-ordinates are correct, the following relation obtained from equation (20) may be useful:

$$\Delta B = \frac{16\pi^2}{n}\frac{\delta_n}{\varrho_n''(0)}\,, \tag{73}$$

where $\delta_n = \varrho_{no}(0) - \varrho_{nc}(0)$, and $\varrho_{no}(0)$ and $\varrho_{nc}(0)$ are the peak heights in the observed and calculated Fourier maps, respectively. $\varrho_n''(0)$ in equation (73) may be taken as the average of $\varrho_{no}''(0)$ and $\varrho_{nc}''(0)$ or may be approximated by $\varrho_{no}''(0)$.

If both atomic co-ordinates and temperature factor deviate slightly from the true values by Δx_n and ΔB, respectively, we may utilize the value of $\partial\delta_n/\partial x_n$ obtained from the difference Fourier maps as follows (cf. Lipson & Cochran, 1953, p. 300):

$$\Delta x_n . \Delta B = -\frac{n}{16\pi^2\delta_n}\frac{\partial\delta_n}{\partial x_n}\,. \tag{74}$$

Equations (73) and (74) will be useful for refinement of the atomic co-ordinates and the temperature factor at the final stage of the structure analysis.

APPENDIX

The incomplete modified Hankel functions are defined by

$$\varkappa_n(2x, y) = \frac{1}{2x^n}\int_y^\infty t^{n-1}\exp\left(-t-\frac{x^2}{t}\right)dt\,, \tag{A-1}$$

and

$$\lim_{y\to 0}\varkappa_n(2x, y) = K_n(2x)\,. \tag{A-2}$$

The series expansion of $\varkappa_0(2x, y)$ and $\varkappa_1(2x, y)$ are as follows. If $x \neq 0$,

$$2\varkappa_0(2x, y) = 2K_0(2x) + Ei\left(-\frac{x^2}{y}\right) - \sum_{n=1}^{\infty}\frac{(-1)^n}{n!}x^{2n}\int_{x^2/y}^\infty\frac{\exp(-t)}{t^{n+1}}dt\,, \tag{A-3}$$

$$2x\varkappa_1(2x, y) = 2xK_1(2x) - \sum_{n=0}^{\infty}\frac{(-1)^n}{n!}x^{2n+2}\int_{x^2/y}^\infty\frac{\exp(-t)}{t^{n+2}}dt\,. \tag{A-4}$$

The integration,

$$I_n = \int_0^\infty\frac{\exp(-bs^2)}{(s^2+p)^n}ds = -\frac{1}{(n-1)}\frac{\partial I_{n-1}}{\partial p}\,, \tag{A-5}$$

appears frequently in our transformation. It may be made to depend on I_1, where

$$I_1 = \frac{\pi\exp(bp)}{2\sqrt{p}}\operatorname{erfc}(\sqrt{(bp)})\,. \tag{A-6}$$

The solution for I_1 may be obtained as follows. Let I_1 be a function of b; then we have

$$\frac{\partial I_1(b)}{\partial b} = -\frac{1}{2}\sqrt{\left(\frac{\pi}{b}\right)} + pI_1(b)\,. \tag{A-7}$$

After multipling by $\exp(-bp)$ on both sides of (A-7), we integrate as follows:

$$\int_b^\infty\frac{\partial}{\partial b}\{\exp(-bp).I_1(b)\}db = -\frac{\sqrt{\pi}}{2}\int_b^\infty\frac{\exp(-bp)}{\sqrt{b}}db\,. \tag{A-8}$$

Equation (A-6) is then easily obtained from (A-8). The function $W(S_0, q_n)$, is also introduced by this procedure.

The author is grateful to Prof. W. N. Lipscomb for his kind interest and to the Office of Ordnance Research for the financial support.

References

Atoji, M. & Lipscomb, W. N. (1953). *Acta Cryst.* **6**, 547.

Atoji, M. & Lipscomb, W. N. (1954). *Acta Cryst.* **7**, 597.

Atoji, M., Lipscomb, W. N. & Wheatley, P. J. (1955). *J. Chem. Phys.* **23**, 1176.

Ayerst, E. M. & Duke, J. R. C. (1954). *Acta Cryst.* **7**, 588.

Berghuis, J., Haanappel, I. M., Potters, M., Loopstra, B. O., McGillavry, H. & Veenedaal, A. L. (1955). *Acta Cryst.* **8**, 478.

Cruickshank, D. W. J. (1949). *Acta Cryst.* **2**, 65.

Drenth, W. & Wiebenga, E. H. (1955). *Acta Cryst.* **8**, 755.

Duncanson, W. E. & Coulson, C. A. (1944). *Proc. Roy. Soc. Edinb.* A, **62**, 37.

Erdélyi, A., Magnus, W., Oberhettinger, F. & Tricomi, F. G. (1954). *Tables of Integral Transforms.* New York: McGraw-Hill.

Higgs, P. W. (1953). *Acta Cryst.* **6**, 232.

International Tables for the Determination of Crystal Structures, (1935). Berlin: Borntraeger.

James, R. W. (1950). *The Optical Principles of the Diffraction of X-rays.* London: Bell.

Ladell, J., McDonald, T. R. R. & Schmidt, G. M. J. (1956). *Acta Cryst.* **9**, 195.

Lipson, H. & Cochran, W. (1953). *The Determination of Crystal Structures.* London: Bell.

Löwdin, Per-Olov (1953). *Phys. Rev.* **90**, 120.

McDonald, T. R. R. (1956). *Acta Cryst.* **9**, 162.

McWEENY, R. (1951). *Acta Cryst.* **4**, 513.
McWEENY, R. (1953). *Acta Cryst.* **6**, 631.
MARGENAU, H. & MURPHY, G. M. (1943). *The Mathematics of Physics and Chemistry*. New York: Van Nostrand.
PAULING, L. & SHERMAN, J. (1932). *Z. Kristallogr.* **81**, 1.
ROSSER, J. B. (1948). *Theory and Application of* $\int_0^z e^{-x^2}dx$ *and* $\int_0^z e^{-p^2y^2}dy \int_0^y e^{-x^2}dx$, part 1. Brooklyn: Mapleton House.
ROZENTAL, S. (1935). *Z. Phys.* **98**, 742.
SAKS, S. (1937). *Theory of the Integral*. New York: Stechert.
SLATER, J. C. (1930). *Phys. Rev.* **36**, 57.
SLATER, J. C. (1932). *Phys. Rev.* **42**, 33.
UMEDA, K. (1951). *J. Fac. Sci. Hokkaido Univ.* (2), **11**, 57.
WATSON, G. N. (1952). *A Treatise on the Theory of Bessel Functions*, 2nd ed. Cambridge: University Press.
WHITTAKER, E. T. & WATSON, G. N. (1935). *A Course of Modern Analysis*, 4th ed. Cambridge: University Press.

Acta Cryst. (1957). **10**, 303

Analytical Representation of Atomic Scattering Factors*

BY V. VAND, P. F. EILAND AND R. PEPINSKY

X-Ray and Crystal Analysis Laboratory, Department of Physics, The Pennsylvania State University, University Park, Pa., U.S.A.

(*Received* 6 *October* 1956)

Atomic scattering factors can be expressed analytically by an expansion of Gaussian functions. A two-term expansion is sufficiently accurate to cover the Cu $K\alpha$ range of scattering angles occurring in crystallographic calculations. For the Mo $K\alpha$ range, one extra constant is to be added.

The constants of the two-term expansion are evaluated for all the elements. The function fits the tabulated atomic scattering factors to better than 1% of $f(0)$ in most cases.

Introduction

The increasing availability of high-speed computers for crystallographic work creates need for analytical expression of atomic scattering factors. We have considered several possible functions for this purpose, and have decided upon a Gaussian expansion

$$f(x) = \sum_j A_j \exp(-a_j x^2), \qquad (1)$$

where $x = \sin\theta$.

This expansion has the advantage of very rapid convergence. If only two terms of the above series are taken, we obtain

$$f(x) = A \exp(-ax^2) + B \exp(-bx^2). \qquad (2)$$

This expression contains only four constants A, B, a, b, which depend on the range to be fitted; two of these are connected by the relation

$$A + B = N, \qquad (3)$$

where N is the number of electrons in the atom or ion. Thus (2) is essentially a three-constant formula. For atoms, $N = Z$, the atomic number; for ions, N differs from Z.

The two-term expansion proved to be sufficiently accurate for all the elements over the whole Cu $K\alpha$ range of angles θ, the error rarely exceeding 1% of $f(0)$. The additional practical advantage is that a subprogram for a Gaussian function is usually already available in the computing routine for the calculation of the temperature factor. A further advantage is that the function has a simple transform, so that computations of electron density and its derivatives are greatly facilitated whenever needed.

Over the Mo $K\alpha$ angular range, the two-term formula gives a poor fit for large angles, and addition of one more term is necessary. It is then sufficient to use a three-term formula:

$$f(x) = A \exp(-ax^2) + B \exp(-bx^2) + C, \qquad (4)$$

with the condition

$$A + B + C = N. \qquad (5)$$

The values of the constants A, B, a, b, are different from the values for the two-term formula.

The only serious disadvantage of the above formulae is that evaluation of the best values of the formula constants is not straightforward. It is a laborious procedure, and least-squares fitting must be done by successive approximations. For this reason only the constants of the two-term expansion have been calculated to date; an IBM 704 program has been designated to evaluate the constants of the three-term expansion.

It should be noted that the use of the Gaussian

* Development supported by Contract No. N6onr-26916, T.O. 16, with the Office of Naval Research, and Grant No. A-228-C from the National Institutes of Health.